This article was downloaded by: [Renmin University of China]
On: 13 October 2013, At: 11:06
Publisher: Taylor & Francis
Informa Ltd Registered in England and Wales Registered Number: 1072954 Registered office: Mortimer House, 37-41 Mortimer Street, London W1T 3JH, UK

Molecular Crystals and Liquid Crystals
Publication details, including instructions for authors and subscription information:
http://www.tandfonline.com/loi/gmcl20

Synthesis and Terminal Chain Effect on the Phase Transition Behavior of Azo-Bridged Benzothiazole-Phenyl Ethers

Arwa Alshargabi [a], Guan-Yeow Yeap [a], Daisuke Takeuchi [b] & Masato M. Ito [c]

[a] Liquid Crystal Research Laboratory, School of Chemical Sciences, Universiti Sains Malaysia, Penang, Malaysia

[b] Chemical Resources Laboratory, Tokyo Institute of Technology, Yokohama, Japan

[c] Department of Environmental Engineering for Symbiosis, Faculty of Engineering, Soka University, Tokyo, Japan

Published online: 22 Apr 2013.

To cite this article: Arwa Alshargabi, Guan-Yeow Yeap, Daisuke Takeuchi & Masato M. Ito (2013) Synthesis and Terminal Chain Effect on the Phase Transition Behavior of Azo-Bridged Benzothiazole-Phenyl Ethers, Molecular Crystals and Liquid Crystals, 575:1, 128-139, DOI: 10.1080/15421406.2013.766919

To link to this article: http://dx.doi.org/10.1080/15421406.2013.766919

PLEASE SCROLL DOWN FOR ARTICLE

Taylor & Francis makes every effort to ensure the accuracy of all the information (the "Content") contained in the publications on our platform. However, Taylor & Francis, our agents, and our licensors make no representations or warranties whatsoever as to the accuracy, completeness, or suitability for any purpose of the Content. Any opinions and views expressed in this publication are the opinions and views of the authors, and are not the views of or endorsed by Taylor & Francis. The accuracy of the Content should not be relied upon and should be independently verified with primary sources of information. Taylor and Francis shall not be liable for any losses, actions, claims, proceedings, demands, costs, expenses, damages, and other liabilities whatsoever or howsoever caused arising directly or indirectly in connection with, in relation to or arising out of the use of the Content.

This article may be used for research, teaching, and private study purposes. Any substantial or systematic reproduction, redistribution, reselling, loan, sub-licensing, systematic supply, or distribution in any form to anyone is expressly forbidden. Terms &

Conditions of access and use can be found at http://www.tandfonline.com/page/terms-and-conditions

Downloaded by [Renmin University of China] at 11:06 13 October 2013

Mol. Cryst. Liq. Cryst., Vol. 575: pp. 128–139, 2013
Copyright © Taylor & Francis Group, LLC
ISSN: 1542-1406 print/1563-5287 online
DOI: 10.1080/15421406.2013.766919

Downloaded by [Renmin University of China] at 11:06 13 October 2013

Synthesis and Terminal Chain Effect on the Phase Transition Behavior of Azo-Bridged Benzothiazole-Phenyl Ethers

ARWA ALSHARGABI,[1] GUAN-YEOW YEAP,[1,*] DAISUKE TAKEUCHI,[2] AND MASATO M. ITO[3]

[1]Liquid Crystal Research Laboratory, School of Chemical Sciences, Universiti Sains Malaysia, Penang, Malaysia
[2]Chemical Resources Laboratory, Tokyo Institute of Technology, Yokohama, Japan
[3]Department of Environmental Engineering for Symbiosis, Faculty of Engineering, Soka University, Tokyo, Japan

A series of azo-bridged benzothiazole-phenyl ethers 4-((6-ethoxybenzothiazol-2-yl)diazenyl)bromoalkoxybenzene in which an exocyclic N=N group is situated between an ethoxy-substituted benzothiazole and a bromoalkoxyphenyl have been synthesized and characterized. The phase transition behavior of these compounds have been correlated against the variation of the flexible alkyl chain with n *methylene units (CH_2), ranging from 5 to 12. The thermal stability as reflected by the transition temperature range of the present homologues is found to be strongly dependent on the length of the CH_2 units. All the members of this series exhibit enantiotropic nematic phases. However, upon further cooling, the compounds with* n = *9–12 also behave as smectogens.*

Keywords Azo-bridged; benzothiazole; ethers; mesogenic; nematic; smectic

1. Introduction

Liquid crystals have been accepted as quintessential materials in our daily life for more than a century. The workability of these materials can be exemplified by their application in technological devices, as prototypical self-organizing molecular materials, as precursor in biological as well as pharmacological fields [1].

In general, these materials possess a mesogenic core, terminal groups and a flexible terminal chain, which are favorable in inducing mesomorphic behavior due to their high shape anisotropy [2–5]. One of these materials contains an azo-based mesogenic core, which has widely been used in optical switching, holography, and optical storage devices [6–11]. The azo-based dyes have also been applied in liquid crystal display (LCD) governed by the guest–host interaction [12]. In addition, the aromatic azo compounds undergo the *cis–trans* isomerization in response to light or heat and thus offer many opportunities in photonic liquid crystals applications [13–15]. Among these compounds, the analogues with

*Address correspondence to Guan-Yeow Yeap, Liquid Crystal Research Laboratory, School of Chemical Sciences, Universiti Sains Malaysia, 11800 Minden, Penang, Malaysia. Tel.: 60-4-6533568; Fax: 60-4-6574854. E-mail: gyyeap@usm.my

Downloaded by [Renmin University of China] at 11:06 13 October 2013

–COO– and –N=N– central bridges have been synthesized and claimed as suitable candidates to exhibit liquid crystal properties [16].

Earlier reports have shown that the introduction of heterocycles greatly influences the mesomorphic properties of the calamitic molecules owing to their unsaturation and more polarizable nature [17]. The effect of heteroatoms (S, O, and N) can change considerably the polarity, polarizability and, sometimes, the geometric shape of the molecule, thereby influencing the type of mesophase, the phase transition temperatures, and the dielectric and other properties of the mesogens [17]. A typical heterocyclic compound is benzothiazole, which could serve as a core unit in calamitic liquid crystals. Prajapati et al. had reported a new mesogenic homologous series containing 6-nitrobenzothiazole and 6-methoxybenzothiazole in which the 6-position in benzothiazole group was substituted by respective nitro and methoxy groups. These compounds with ether and ester linkages on the other side of the azo seem to show enantiotropic nematic (N) and smectic A (SmA) phases [18,19].

A recent finding by our group has shown that the azo-bridged benzothiazole-phenyl esters favor the formation of the N phase [20]. The 2,6-di-substituted benzothiazole was preferred over 2,5-di-substituted analogues due to its linearity [21] and thermal stability [22].

The present study focuses on 2,6-di-substituted benzothiazole in which the bromoalkoxyphenyl will be linked to the 2-position of the 6-ethoxy-benzothiazole via the N=N azo bond. The synthetic route used for the preparation of **1** and **2a–2g** is summarized in Scheme 1.

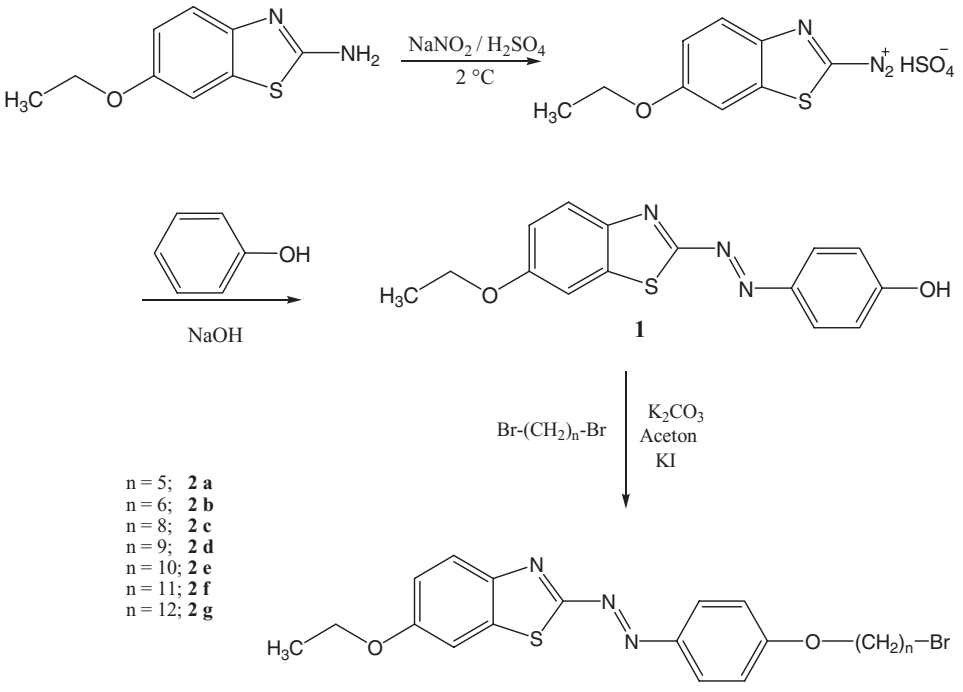

Scheme 1. Synthetic route to formation of the compounds **2a–2g**.

2. Experimental

2.1. Materials

2-amino-6-ethoxybenzothiazole and dibromoalkane ($C_nH_{2n}Br_2$, where $n = 5$, 6, 8, 9, 10, 11, and 12) were purchased from Acros Organics and TCI. Sodium nitrite and phenol were obtained from M&R and Sigma, respectively. All of the reagents and solvents were used without further purification.

2.2. Measurements

CHN microanalysis was carried out on the Perkin Elmer 2400 LS Series CHNS/O analyzer. The infrared (IR) spectra for all intermediates and final compounds were recorded using the Perkin Elmer 2000 FT-IR spectrophotometer, in which the samples were prepared as KBr disks. ^{1}H-NMR (nuclear magnetic resonance) as well as ^{13}C-NMR spectra were recorded in $CDCl_3$ and deuterated DMSO using a Bruker 500 MHz Ultrashield^{TM} FT-NMR spectrometer. Tetramethylsilane (TMS) was used as an internal standard.

The phase transition temperature and associated enthalpy values were determined using a differential scanning calorimeter (DSC) (Seiko DSC6200R), in which the samples were heated and cooled at the rates of $\pm 5^\circ$C min^{-1}. Texture observation of the mesophase was carried out by using polarizing optical microscopy (POM) (Carl Zeiss Axioskop 40 polarizing microscope) equipped with a hot stage (Linkam LTS350) and a temperature controller (TMS94).

2.3. Synthesis

*2.3.1. Synthesis of 4-((5-ethoxybenzothiazol-2-yl)diazenyl)phenol (**1**).* A solution containing 20 ml diluted sulphuric acid (60%) and 6-ethoxy-2-aminobenzothiazole (1 g, 5.1 mmol), which was earlier dissolved in 15 ml glacial acetic acid, was cooled down to 5°C. Sodium nitrite (0.35 g, 5.1 mmol) in 12.5 ml water was added dropwise to the cooled mixture and stirred for 1 h in an ice bath. Phenol (0.47 g, 5.1 mmol) dissolved in 15 ml ethanol was cooled to 5°C and the diazonium salt solution was added dropwise at a temperature below 5°C. The mixture was stirred for 1 h. The pH was subsequently increased to 6–7 by the addition of 1 N NaOH and the mixture was stirred for 1 h in an ice bath. Finally, water was added to the resulting mixture and the precipitate was collected by filtration. The product was recrystallized from ethanol. Yield (70.4%) as red crystals and m.p. 286–287°C. IR (KBr) ν_{max}/cm^{-1}: 3300–2600 (OH broad), 3042 (C–H aromatic), 1605, 1579 (C=C aromatic, C=N thiazole), 2943 (C–H aliphatic), 1057 (bezothiazole), 1135 (C–O). ^{1}H-NMR (DMSO-d_6) δ/ppm: 1.39 (t, 3H, –CH_3), 4.1 (q, 2H, –OCH_2), 7.01 (d, 2H, ArH), 7.1 (d, 1H, ArH), 7.6 (d, 1H, ArH), 7.8 (d, 2H, Ar), 8.0 (s, 1H, ArH).

*2.3.2. Synthesis of 4-((6-ethoxybenzothiazol-2-yl)diazenyl) bromo-alkoxyphenyl (**2a–2g**).* A mixture consisting of compound **1** (8.33 mmol) in 150 ml dry acetone, potassium carbonate (K_2CO_3) (62 mmol), a catalytic amount of potassium iodide (100 mg), and a five-fold excess of dibromoalkane (41.6 mmol) was refluxed for 24 h. K_2CO_3 was removed by filtration while it was still hot and the acetone was removed under reduced pressure. The product was recrystallized three times from ethanol whereupon the pure compound was isolated.

Downloaded by [Renmin University of China] at 11:06 13 October 2013

Downloaded by [Renmin University of China] at 11:06 13 October 2013

The analytical data, IR, ^{1}H-NMR, and ^{13}C-NMR spectra data for **2a–2g** are summarized as follows:

2a: Yield 53.5%. Orange. Elemental analysis (%): Found C 53.51, H 4.93, N 9.36; calculated ($C_{20}H_{22}BrN_3O_2S$) C 53.57, H 4.95, N 9.37. IR (KBr) ν_{max}/cm^{-1}: 3071 (C–H aromatic), 2975, 2865 (C–H aliphatic), 1600 (C=C aromatic), 1578 (C=N, thiazole), 1263 (Ar–O–R ether), 1053 (C–S–C, thiazole). ^{1}H-NMR (500 MHz, $CDCl_3$) δ/ppm: 1.47 (t, 3H, CH_3–), 1.53–1.55 (m, 2H, –$(CH_2)_2$–), 1.8–1.9 (m, 4H, – $(CH_2)_2$–), 3.46 (t, 2H, –CH_2Br), 4.09–4.14 (m, 4H, (CH_2)O–), 7.01 (d, 2H, Ar–H), 7.08 (d-d, 1H, Ar–H), 7.26 (d, 1H, Ar–H), 7.9 (s, 1H, Ar–H), 8.0 (d, 2H, Ar–H). ^{13}C-NMR ($CDCl_3$) δ/ppm: 173.88 (C=N), 163.39–105.02 (Ar–C), 68.15 (O–$\underline{CH_2}$–CH_3), 64.15 (O–$\underline{CH_2}$–CH_2), 33.49 (–$\underline{CH_2}$Br), 32.4–24.76 (–$(CH_2)_3$–), 14.79 (–CH_3).

2b: Yield 64.7%. Orange. Elemental analysis (%): Found C 54.3, H 5.19, N 9.0; calculated ($C_{21}H_{24}BrN_3O_2S$) C 54.5, H 5.2, N 9.0. IR (KBr) ν_{max}/cm^{-1}: 3071 (C–H aromatic), 2981, 2868 (C–H aliphatic), 1599 (C=C aromatic), 1577 (C=N, thiazole), 1261 (Ar–O–R ether), 1056 (C–S–C, thiazole). ^{1}H-NMR (500 MHz, $CDCl_3$) δ/ppm: 1.47 (t, 3H, CH_3–), 1.53–1.55 (m, 4H, –$(CH_2)_2$–), 1.8–1.9 (m, 4 H, – $(CH_2)_2$–), 3.45 (t, 2H, –CH_2Br), 4.09–4.13 (m, 4H, $(CH_2)_2$O–), 7.01 (d, 2H, Ar–H), 7.07 (d-d, 1H, Ar–H), 7.29 (d, 1H, Ar–H), 8.0 (s, 1H, Ar–H), 8.0 (d, 2H, Ar–H). ^{13}C-NMR ($CDCl_3$)/δ: 173.89 (C=N), 163.49–105.01 (Ar–C), 68.29 (O–$\underline{CH_2}$–CH_3), 64.14 (O–$\underline{CH_2}$–CH_2), 33.75 (–$\underline{CH_2}$Br), 32.62–25.0 (–$(CH_2)_4$–), 14.78 (–CH_3).

2c: Yield 62.5%. Orange. Elemental analysis (%): Found C 55.86, H 4.73, N 8.51; calculated ($C_{23}H_{28}BrN_3O_2S$) C 56.32, H 4.75, N 8.57. IR (KBr) ν_{max}/cm^{-1}: 3071 (C–H aromatic), 2925, 2860 (C–H aliphatic), 1601 (C=C aromatic), 1578 (C=N, thiazole), 1263 (Ar–O–R ether), 1050 (C–S–C, thiazole). ^{1}H-NMR (500 MHz, $CDCl_3$) δ/ppm: 1.39 (t, 3H, CH_3–), 1.47–1.45 (m, 8H, –$(CH_2)_4$–), 1.83–1.87 (m, 4H, –$(CH_2)_2$–), 3.42 (t, 2H, –CH_2Br), 4.07–4.14 (m, 4H, $(CH_2)_2$O–), 7.01 (d, 2H, Ar–H), 7.08 (d-d, 1H, Ar–H), 7.29 (d, 1H, Ar–H), 8.0 (s, 1H, Ar–H), 8.1 (d, 2H, Ar–H). ^{13}C-NMR ($CDCl_3$) δ/ppm: 173.92 (C=N), 163.59–105.03 (Ar–C), 68.51 (O–$\underline{CH_2}$–CH_3), 64.15 (O–$\underline{CH_2}$–CH_2), 33.89 (–$\underline{CH_2}$Br), 33.47–25.89 (–$(CH_2)_6$–), 14.79 (–CH_3).

2d: Yield 62.3%. Orange. Elemental analysis (%): Found C 56.97, H 5.88, N 8.42; calculated ($C_{24}H_{30}BrN_3O_2S$) C 57.14, H 5.99, N 8.33. IR (KBr) ν_{max}/cm^{-1}: 3071 (C–H aromatic), 2926, 2855 (C–H aliphatic), 1596 (C=C aromatic), 1578 (C=N, thiazole), 1261 (Ar–O–R ether), 1052 (C–S–C, thiazole). ^{1}H-NMR (500 MHz, $CDCl_3$) δ/ppm: 1.5 (t, 3H, CH_3–), 1.39–1.47 (q, 10H, –$(CH_2)_5$–), 1.83–1.87 (m, 4H, –$(CH_2)_2$–), 3.41 (t, 2H, –CH_2Br), 4.07–4.14 (m, 4H, $(CH_2)_2$O–), 7.0 (d, 2H, Ar–H), 7.07 (d-d, 1H, Ar–H), 7.29 (d, 1H, Ar–H), 7.9 (s, 1H, Ar–H), 8.0 (d, 2H, Ar–H). ^{13}C-NMR ($CDCl_3$) δ/ppm: 173.92 (C=N), 163.63–105.03 (Ar–C), 68.55 (O–$\underline{CH_2}$–CH_3), 64.15 (O–$\underline{CH_2}$–CH_2), 34.03 (–$\underline{CH_2}$Br), 29.50–25.94 (–$(CH_2)_7$–), 14.79 (–CH_3).

2e: Yield 65.8%. Orange. Elemental analysis (%): Found C 57.61, H 6.19, N 8.04; calculated ($C_{25}H_{32}BrN_3O_2S$) C 57.91, H 6.22, N 8.10. IR (KBr) ν_{max}/cm^{-1}: 3077 (C–H aromatic), 2980, 2851 (C–H aliphatic), 1598 (C=C aromatic), 1579 (C=N, thiazole), 1262 (Ar–O–R ether), 1058 (C–S–C, thiazole). ^{1}H-NMR (500 MHz, $CDCl_3$) δ/ppm: 1.49 (t, 3H, CH_3–), 1.32–1.47 (q, 12H, –$(CH_2)_6$–), 1.83–1.89 (m, 4H, –$(CH_2)_2$–), 3.41 (t, 2H, –CH_2Br), 4.0–4.1 (m, 4H, $(CH_2)_2$O–), 7.0 (d, 2H, Ar–H), 7.1 (d-d, 1H, Ar–H), 7.29 (d, 1H, Ar–H), 7.9 (s, 1H, Ar–H), 8.1 (d, 2H, Ar–H). ^{13}C-NMR ($CDCl_3$) δ/ppm: 173.92 (C=N), 163.61–105.02 (Ar–C), 68.56 (O–$\underline{CH_2}$–CH_3), 64.14 (O–$\underline{CH_2}$–CH_2), 34.06 (–$\underline{CH_2}$Br), 33.47–25.89 (–$(CH_2)_8$–), 14.79 (–CH_3).

2f: Yield 64.7%. Orange. Elemental analysis (%): Found C 58.30, H 6.46, N 7.93; calculated ($C_{26}H_{34}BrN_3O_2S$) C 58.64, H 6.44, N 7.89. IR (KBr) ν_{max}/cm^{-1}: 3071

(C–H aromatic), 2938, 2851 (C–H aliphatic), 1597 (C=C aromatic), 1578 (C=N, thiazole), 1261 (Ar–O–R ether), 1058 (C–S–C, thiazole). ^{1}H-NMR (500 MHz, $CDCl_3$) δ/ppm: 1.48 (t, 3H, CH_3–), 1.38–1.43 (q, 14H, –$(CH_2)_7$–), 1.81–1.84 (m, 4H, –$(CH_2)_2$–), 3.39 (t, 2H, –CH_2Br), 4.05–4.12 (m, 4H, $(CH_2)_2$O–), 7.01 (d, 2H, Ar–H), 7.07 (d-d, 1H, Ar–H), 7.29 (d, 1H, Ar–H), 7.98 (s, 1H, Ar–H), 8.0 (d, 2H, Ar–H). ^{13}C-NMR ($CDCl_3$) δ/ppm: 173.92 (C=N), 163.62–105.02 (Ar–C), 68.58 (O–$\underline{CH_2}$–CH_3), 64.14 (O–$\underline{CH_2}$–CH_2), 34.07 (–$\underline{CH_2}$Br), 33.54–25.95 (–$(CH_2)_9$–), 14.79 (–CH_3).

2g: Yield 69.9%. Orange. Elemental analysis (%): Found C 59.31, H 6.65, N 7.66; calculated ($C_{27}H_{36}BrN_3O_2S$) C 59.33, H 6.64, N 7.69. IR (KBr) ν_{max}/cm^{-1}: 3071 (C–H aromatic), 2938, 2851 (C–H aliphatic), 1597 (C=C aromatic), 1578 (C=N, thiazole), 1261 (Ar–O–R ether), 1058 (C–S–C, thiazole). ^{1}H-NMR (500 MHz, $CDCl_3$) δ/ppm: 1.48 (t, 3H, CH_3–), 1.38–1.48 (m, 16H, –$(CH_2)_8$–), 1.8–1.9 (m, 4H, – $(CH_2)_2$–), 3.45 (t, 2H, –CH_2Br), 4.09–4.13 (m, 4H, $(CH_2)_2$O–), 7.01 (d, 2H, Ar–H), 7.07 (d-d, 1H, Ar–H), 7.29 (d, 1H, Ar–H), 8.0 (s, 1H, Ar–H), 8.1 (d, 2H, Ar–H). ^{13}C-NMR ($CDCl_3$) δ/ppm: 173.93 (C=N), 163.64–105.03 (Ar–C), 68.60 (O–$\underline{CH_2}$–CH_3), 64.14 (O–$\underline{CH_2}$–CH_2), 33.89 (–$\underline{CH_2}$Br), 33.55–25.96 (–$(CH_2)_{10}$–), 14.79 (–CH_3).

3. Results and Discussion

3.1. Mesomorphic Behavior

The phase transition temperatures and corresponding enthalpy changes of compounds **2a–2g** determined by DSC are summarized in Table 1. All compounds in this series show enantiotropic N phase. However, compounds **2d–2g** also exhibit monotropic SmA phase.

Table 1. Phase transition temperatures (°C) and enthalpies (in kJ mol^{-1}) for **2a–2g**. (Cr: crystal; SmA: smectic A; N: nematic; I: isotropic)

Compound	Transition temperatures (°C) (ΔH, kJ mol^{-1}): Heating cooling
2a	Cr 132.6 (42.5) N 145.4 (0.7) I
	I 143[a] N 84.7 (14.0) Cr
2b	Cr 109.9 (39.9) N 143.9 (1.0) I
	I 135[a] N 77 Cr1 46.5 (5.2) Cr2
2c	Cr 107.0 (43.8) N 138.8 (0.9) I
	I 138[a] N 80 (24.7) Cr
2d	Cr 120.6 (48.3) N 135.4 (0.8) I
	I 122.6 (0.5) N 87.8 (0.4) SmA 74.0
2e	(22.5) Cr
	Cr 106.7 (47.4) N 130.8 (0.9) I
2f	I 119.1 (0.7) N 89.5 (0.6) SmA 73.6
	(30.5) Cr
2g	Cr 102.1 (37.6) N 128.3 (1.0) I
	I 121.6 (0.8) N 93.5 (1.2) SmA 62.2 (25.2) Cr
	Cr 97.4 (29.4) N 119.3 (0.7) I
	I 113.6 (0.7) N 89.6 (1.1) SmA 73.6 (24.2) Cr

[a]Denotes transition temperatures determined via polarizing optical microscopy, but undetected via DSC.

Downloaded by [Renmin University of China] at 11:06 13 October 2013

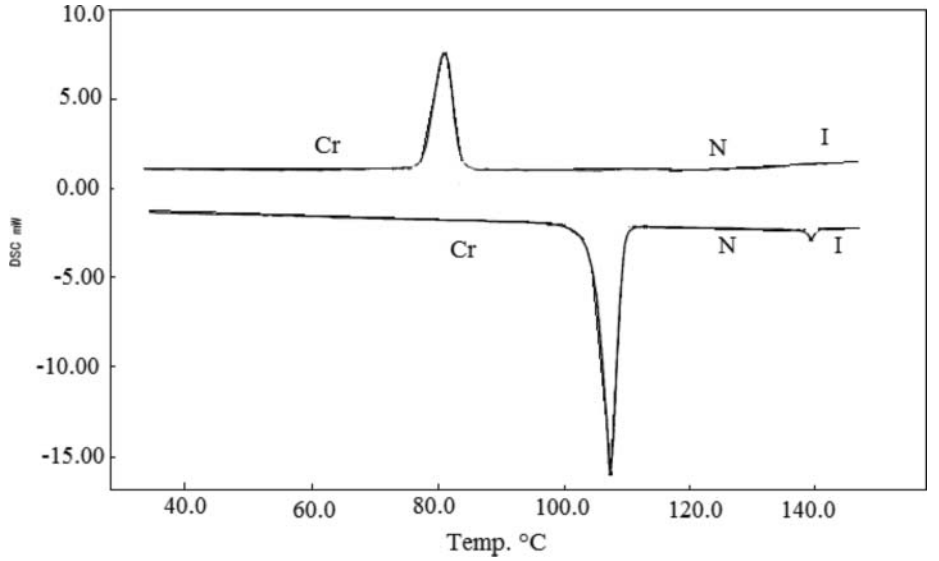

Figure 1. Differential scanning calorimetry (DSC) thermogram of **2c** during heating and cooling scans.

The DSC thermograms of **2c** and **2e** during heating and cooling scans are shown in Figs 1 and 2, respectively. From Fig. 1, on heating, the DSC curve for compound **2c** shows two endothermic peaks at 107°C and 138.8°C, which represent the Cr–N and N–I transitions, respectively.

However, on cooling, the DSC curve for compound **2e** shows three exothermic peaks at 119.1°C, 89.5°C, and 73.6°C, which can be assigned to the I–N, N–SmA and SmA–Cr transitions, respectively (Fig. 2).

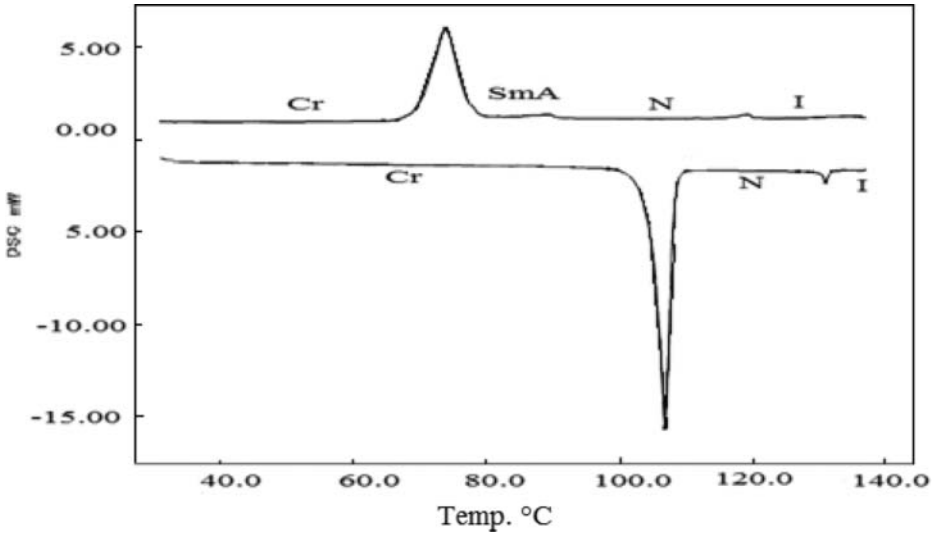

Figure 2. DSC thermograms of **2e** upon heating and cooling.

Downloaded by [Renmin University of China] at 11:06 13 October 2013

The mesophases for all the compounds are observed under a POM during heating and cooling cycles. One of the notable features is that the compounds **2a–2c** exhibit predominant enantiotropic N phase, while **2d–2g** exhibit monotropic SmA as well as enantiotropic N phases.

Observation on cooling **2e** from its isotropic (I) liquid phase shows the presence of two mesophases. Initial cooling from the I liquid phase led to nematic droplets (Fig. 3(a)), which appear and coalesce to form the typical schlieren texture with disclination lines (Fig. 3(b)). Upon further cooling of the N phase, the emergence of the SmA phase is observed at 89.5°C (Fig. 3(c)). All the observed liquid-crystalline textures resemble those reported in the literature [23,24].

3.2. Structure–Mesomorphic Property Relationships

While Fig. 4 represents the correlation of transition temperatures with the number of carbons in the terminal bromoalkoxyl chain of **2a–2g** during the heating cycle, Fig. 5 illustrates the thermal stability of mesophase upon the cooling cycle for the same series.

The thermogram indicates that the length of the bromoalkoxy chain also influences the types of mesophase. The odd-even effect on the mesomorphic properties is not obvious, but it can still be noted when moving from **2c** to **2e** (Fig. 4). According to the plot, the clearing (N–I) point shows a descending trend from **2a** (145.4°C) to **2g** (119.3°C), while the melting point (Cr–N) shows a slight increment for **2d** (120.6°C) and again descending from **2e** (106.7°C) to **2g** (79.4°C). This behavior is due to the flexible terminal chain, which acts as a diluent to the mesogenic core ring system, and hence depressed both the melting and the clearing temperature of this series [25,26].

It is also important to mention that upon increasing the number of carbon in the C_nH_{2n} unit, a significant decrease in the N phase temperature range (ΔN) is observed for all the members and an increase in the phase stability of the SmA phase in **2d–2g**.

By referring to the graph in Fig. 5, ΔN has apparently decreased by the increase in the length of the terminal chain from 58.3°C for **2a** to 24°C for **2g**. This phenomenon results from the long terminal chain being attracted and intertwined, which in turn facilitates lamellar packing, causing a decrease in ΔN [27,28]. Generally, members with shorter terminal chain favor the formation of the N phase, whereas the smectic phase is more favorable by members having longer chain [25]. However, Fig. 5 also indicates that the SmA phase temperature range (ΔSmA) was found to be 13.8°C for **2d**, and with an additional methylene unit, the ΔSmA increases from 15.9°C to 31.3°C for **2e** and **2f**, respectively, and then decreases to 16°C for **2g**.

3.3. Spectroscopic Studies

The IR and NMR spectra obtained for all compounds in this series have shown similar characteristics as those recorded for compound **2b**. Hence, the characterization based on compound **2b** will be described.

From the FTIR (Fourier transform infrared spectroscopy) spectrum, the diagnostic absorption bands resulting from the alkyl groups are observed at 2868 and 2981 cm^{-1}. The relative intensity of the absorption bands of the alkyl groups increased upon ascending the series due to the increasing number of carbons in the alkoxyl chain. The absorption bands assignable to the stretching of the C=N and C=C bonds in benzothiazole are observed at 1577 and 1599 cm^{-1}, respectively. The absorption band observed at 1261 cm^{-1} is indicative of the C–O stretching of the aromatic ether Ar–O–R.

Downloaded by [Renmin University of China] at 11:06 13 October 2013

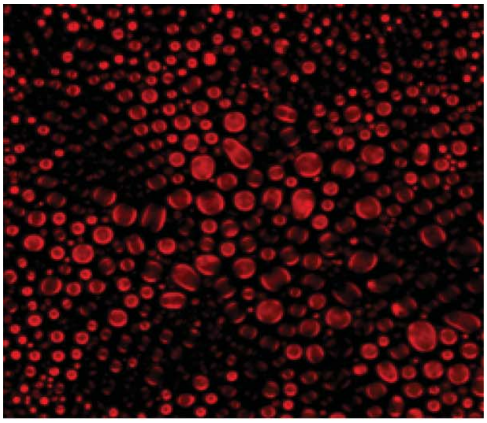

(a)

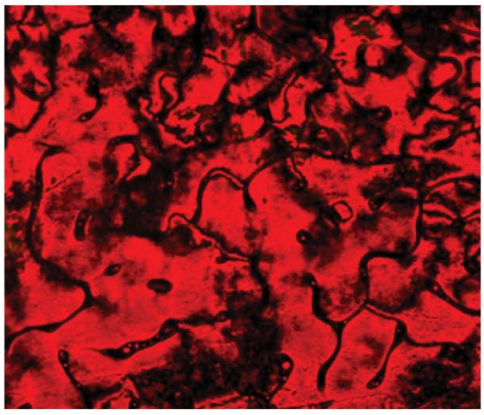

(b)

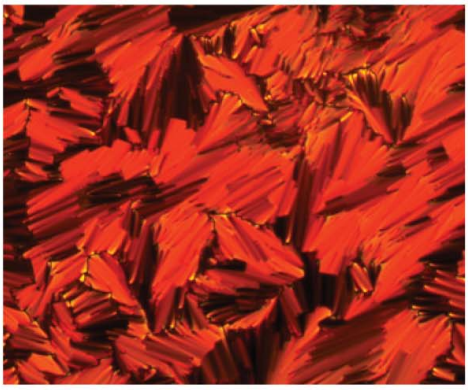

(c)

Figure 3. Optical photomicrographs of **2e**. Upon cooling from the isotropic liquid, nematic droplets (a) appeared and coalesced to form the typical schlieren texture (b). On further cooling, SmA phase shown in (c) was observed.

Downloaded by [Renmin University of China] at 11:06 13 October 2013

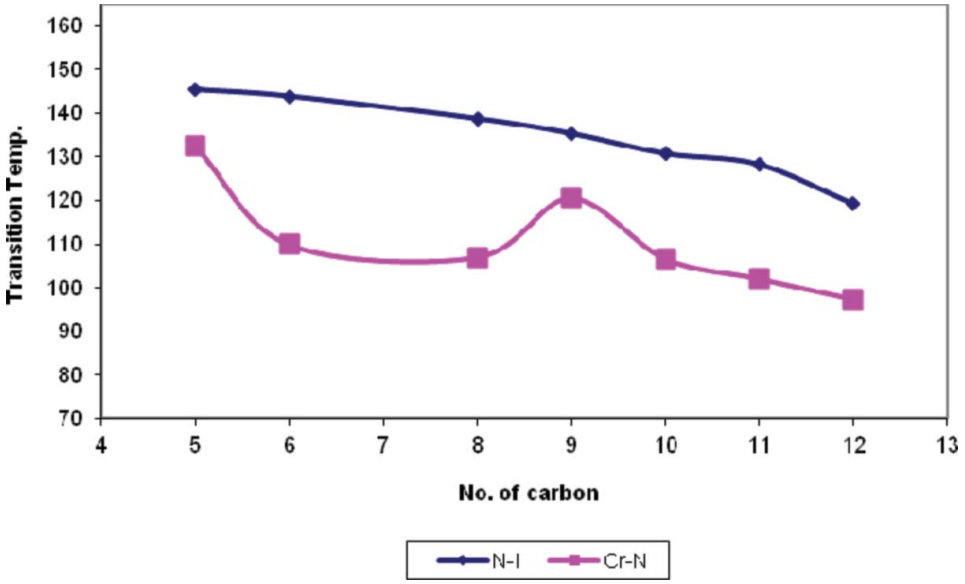

Figure 4. Dependence of the transition temperatures on the number of methylene units in the terminal bromoalkoxyl chains for **2a–2g**.

The ^{1}H-NMR data for compound **2b** show a triplet at δ 1.47 ppm, indicating that the methyl protons from the ethoxy group attached to the benzothiazole. All the methylene protons from the bromo-substituted terminal chain, except those from the carbons attached directly to O and Br, gave multiplets at δ 1.53–1.55 ppm. The presence of a quintet at δ 1.7 ppm can be assigned to the methylene protons in –$\underline{CH_2}$–CH_2–O– and –$\underline{CH_2}$–CH_2–Br. Both triplet (δ 3.45 ppm) and quadruplet (δ 4.10 ppm) can be assigned to the protons of –$\underline{CH_2}$Br and –O$\underline{CH_2}$– originating from the same terminal chain.

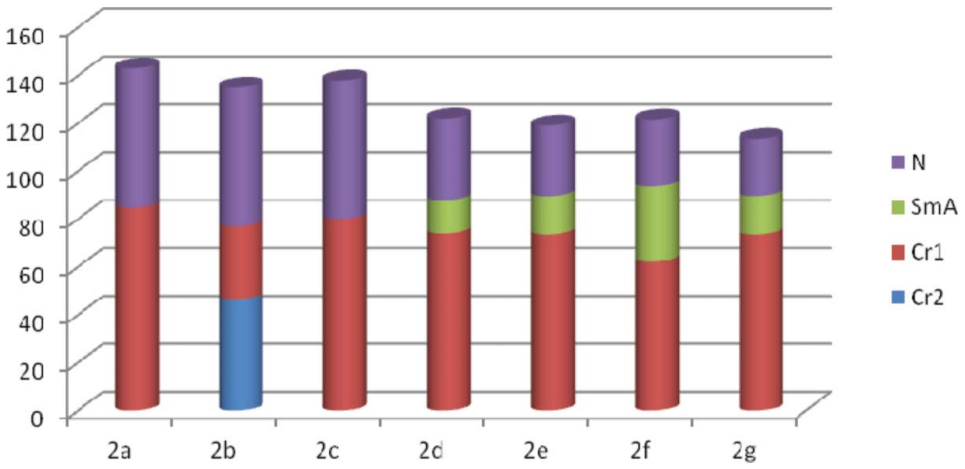

Figure 5. Graphical representations of the phase transition temperature ranges for **2a–2g**.

Downloaded by [Renmin University of China] at 11:06 13 October 2013

The diagnostic peaks as inferred from the ^{13}C-NMR spectrum for **2b** has supported the presence of 21 carbons within this molecule. The peak at δ 173.89 is due to the C=N, which formed part of the heterocyclic ring of benzothiazole. The resonances observed at δ 105.01–163.49 ppm support the presence of the remaining sp^2 carbons in benzothiazole and aromatic units. While the resonance observed at δ 14.78 ppm supports the presence of a methyl carbon from the ethoxy group, the peaks within the range of δ 25.0–31.62 ppm are indicative of the methylene carbons that are not bonded directly to O and Br within the terminal chain. However, the more downfield peaks at δ 33.75 ppm and 68.29 ppm can be ascribed to the carbon attached to Br and O, respectively. On the other hand, the downfield resonance recorded at δ 64.14 ppm can be assigned to the carbon attached to the oxygen in the ethoxy group.

Downloaded by [Renmin University of China] at 11:06 13 October 2013

3.4. Comparison Studies Between Title Compounds with 4-((6-Ethoxybenzothiazol-2-yl)Azenyl)Phenylalkanoate n*EBTHDZ*

A comparison of the title compound with the recently reported benzothiazole ***n*EBTHDZ** [20] has been carried out. The purpose of making this comparison is based on the fact that the presence of an ether linkage, along with the existence of a terminal Br atom, gives rise to appreciable change in mesomorphic properties. The illustrations of the molecular structure for the title compound and ***n*EBTHDZ** show that these compounds possess a benzothiazole moiety attached to the N atom of the azo group, while the other N of the azo group is attached by a phenyl ring in which the *para* position consists of a Br-substituted alkyloxy chain linked to the phenyl ring via ether linkage.

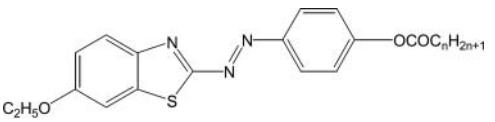

***n*EBTHDZ**

where n = 9 and 10

9EBTHDZ Cr 106.8 (38.8) N 137.7 (1.2) I 139.2 (0.9) N 76.1 (38.8) Cr
11EBTHDZ Cr 106.5 (40) N 132.5 (0.9) I 131.3 (0.9) N 77.9 (40.7) Cr

Compounds with alkyl chain of **9EBTHDZ** and **11EBTHDZ** are purely nematogenic, while the compounds **2d** and **2f** exhibit enantiotropic N phase along with monotropic SmA phase. The presence of SmA in **2d** and **2f** is due to (i) the presence of an ether-linking group that provides greater linearity to molecules rather than the presence of an ester group, and (ii) in terms of van der Waals radii, the Br atom is larger than the H atom. Besides, the polar Br atom increases the molecular polarizability because the valence electrons of this atom are positioned far apart from the nucleus [29]. However, the thermal stability of the N phase for compound **9EBTHDZ** is higher by 16.1°C than that for compound **2d**. In addition, **11EBTHDZ** possesses higher clearing temperature of 132.5°C in comparison with **2f**, owing to the π-electrons associated with the carbonyl group, which provides greater intermolecular interactions among molecules [30].

4. Conclusion

A series of 4-((6-ethoxybenzothiazol-2-yl)diazenyl)bromoalkoxyphenyl has been synthesized and characterized. All the target compounds exhibit enantiotropic N phase. However, on further cooling, **2d–2g** also show monotropic SmA phase.

The varying length of the terminal bromoalkoxyl chain is one of the determining factors that affects the melting and clearing temperatures. The melting temperatures decrease when the length increases from **2a** to **2g**, except for compound **2d**. Similarly, the clearing temperatures also decrease from **2a** to **2g** with the elongation of the molecule. It is noteworthy to mention that the smectogenic properties will be observed only when the compounds possess longer terminal chain (**2d–2g**).

Downloaded by [Renmin University of China] at 11:06 13 October 2013

Acknowledgment

The main author (G-Y. Yeap) would like to thank Universiti Sains Malaysia for funding the project through an FRGS (Fundamental Research Grant Scheme) grant (account no. 203/PKIMIA/6711192).

References

[1] Goodby, J. W. (2007). *Chem Soc. Rev.*, *36*, 1855–1856.
[2] Imrie, C. T., & Henderson, P. A. (2002). *J. Colloid Interface Sci.*, *7*, 298–311.
[3] Yoshizawa, A., Kinbara, H., Narumi, T., Yamaguchi, A., & Dewa, H. (2005). *Liq. Cryst.*, *32*, 1175–1181.
[4] Imrie, C. T., & Luckhurs, G. R. (1998). *J. Mater. Chem.*, *8*, 1339–1343.
[5] Gray, G. W. (1987). *Thermotropic Liquid Crystals*, John Wiley: Chichester.
[6] Ruslim, C., & Ichimura, K. (1999). *J. Mater. Chem.*, *9*, 673–681.
[7] Belmar, J., Parra, M., Zuniga, C., Perez, C., Munoz, C., Omenat, A., & Serrano, J. (1999). *Liq. Cryst.*, *26*, 389–396.
[8] Lai, L. L., Wang, E., Liu, Y. H., & Wang, Y. (2002). *Liq. Cryst.*, *29*, 871–875.
[9] Prajapati, A. K. (2001). *Mol. Cryst. Liq. Cryst.*, *364*, 769–777.
[10] Komitov, L., Ichimura, K., & Strigazz, A. (2000). *Liq. Cryst.*, *27*, 51–55.
[11] Komitov, L., Ruslim, C., Matsuzawa, Y., & Ichimura, K. (2000). *Liq. Cryst.*, *27*, 1011–1016.
[12] Matsui, M., Nakagaway, Y. H., Joglekary, B., Shibatay, K., Muramatsuy, H., Abe, Y., & Kanekos, M. (1996). *Liq. Cryst.*, *21*, 669–682.
[13] Ichimura, K. (2000). *Chem. Rev.*, *100*, 1847–1873.
[14] Ikeda, T. J. (2003). *Mater. Chem.*, *13*, 2037–2057.
[15] Thaker, B. T., & Kanojiya, J. B. (2011). *Liq. Cryst.*, *38*, 1035–1055.
[16] Doshi, A. V., & Makwanaa, N. G. (2011). *Der Pharma Chemica.*, *3*, 580–587.
[17] Lai, L. L., Wang, C. H., Hsien, W. P., & Lin, H. C. (1996). *Mol. Cryst. Liq. Cryst.*, *287*, 177–181.
[18] Prajapati, A. K., & Bonde, N. L. (2006). *J. Chem. Sci.*, *118*, 203–210.
[19] Prajapati, A. K., & Bonde, N. L. (2009). *Mol. Cryst. Liq. Cryst.*, *501*, 72–85.
[20] Yeap, G. Y., Alshargabi, A., Ito, M. M., Mahmood, W. A. K., & Takeuchi, D. (2012). *Mol. Cryst. Liq. Cryst.*, *557*, 126–133.
[21] Aldred, M. P., Vlachos, P., Dong, D., Kitney, S. P., Tsoi, W. C., O'Neill, M., & Kelly, S. M. (2005). *Liq. Cryst.*, *32*, 951–965.
[22] Pavluchenko, A. I., Smirnova, N. I., Titov, V. V., Kovahev, E. I., & Djumaev, K. M. (1976). *Mol. Cryst. Liq. Cryst.*, *37*, 35–46.
[23] Demus, D., & Richter, L. (1987). *Textures of Liquid Crystals*, Verlag Chemie: New York.
[24] Dierking, I. (2003). *Textures of Liquid Crystals*, Wiley-VCH: Weinheim.
[25] Collings, P. J., & Hird, M. (1998). *Introduction to Liquid Crystals: Chemistry and Physics*, Taylor & Francis: London.

[26] Berdague, P., Bayle, J. P., Ho, M. S., & Fung, B. M. (1993). *Liq. Cryst.*, *14*, 667–674.
[27] Yeap, G. Y., Ha, S. T., Lim, P. L., Boey, P. L., Ito, M. M., Sanehisa, S., & Youhei, Y. (2006). *Liq. Cryst.*, *33*, 205–211.
[28] Ha, S. T., Koh, T. M., Lee, S. L., Yeap, G. Y., Lin, H. C., & Ong, S. T. (2010). *Liq. Cryst.*, *37*, 547–554.
[29] Yeap, G. Y., Lee, H. C., Mahmood, W. A. K., Imrie, C. T., Takeuchi, D., & Osakada, K. (2011). *Phase Trans.*, *84*, 29–37.
[30] Ha, S. T., Ong, L. K., Sivasothy, Y., Yeap, G. Y., Lin, H. C., Lee, S. L., Boey, P. L., & Bonde, N. L. (2010). *Int. J. Phys. Sci.*, *5*, 564–575.

Downloaded by [Renmin University of China] at 11:06 13 October 2013